

# Numerical modeling of multidimensional problems of gravitational gas dynamics with high resolution schemes

Boris Rybakin, Natalia Shider

**Abstract.** The aim of this paper is to implement and analyze a nonoscillatory high-resolution scheme for multidimensional hyperbolic conservation laws. Using methods of Nessyahu and Tadmor for solving three-dimensional equations of gravitational gas dynamics we provide a central two-step (predictor and corrector) scheme.

**Mathematics subject classification:** 34C05, 58F14.

**Keywords and phrases:** Mathematical modeling, gravitational gas dynamics, astrophysics.

## 1 Introduction

High resolution numerical schemes are used to solve multidimensional problems of gravitational gas dynamics. Most of modern cosmological models assume existence of two matter types in the Universe – baryonic matter and another one known as a dark matter. The first may be straight examined and includes atoms of any sort. The second one is undetectable by its emitted radiation, but its presence can be inferred from gravitational effects on visible matter. Gaseous nebula is considered to be a formation of gas, dust and other materials that "clump" together to form larger masses, which attract further matter, and eventually become big enough to form stars. The remaining materials are then believed to form planets, and other planetary system objects [1, 2]. For a sufficiently accurate description of these problems we need to apply high-resolution difference schemes which use high-order schemes. A stable calculation in presence of shock waves requires a certain amount of numerical dissipation, in order to avoid the formation of unphysical numerical oscillations [3].

A three-dimensional difference scheme of the type TVD and some other related results are presented in the paper [4].

## 2 Governing Equations

The equations of a self-gravitational ideal hydrodynamics may be expressed in a conservative form with a source term:

$$\frac{\partial \mathbf{U}}{\partial t} + \frac{\partial \mathbf{F}_x}{\partial x} + \frac{\partial \mathbf{F}_y}{\partial y} + \frac{\partial \mathbf{F}_z}{\partial z} = 0, \quad (1)$$

together with Poissons equation

$$\nabla^2 \Phi = 4\pi G \rho, \quad (2)$$

here  $\mathbf{U}$  is a vector of conservative variables;  $\mathbf{F}_x$ ,  $\mathbf{F}_y$  and  $\mathbf{F}_z$  are numerical fluxes. In equation (2)  $\Phi$ ,  $G$  and  $\rho$  denote respectively the gravitational potential, the gravitational constant and the density.

Equation (1) for ideal gas with self-gravity  $\mathbf{U}$  is expressed in terms of

$$\mathbf{U} = (\rho, \rho \mathbf{v}_x, \rho \mathbf{v}_y, \rho \mathbf{v}_z, \rho \mathbf{E})^T, \quad (3)$$

$$\mathbf{F}_x = \begin{pmatrix} \rho v_x \\ \rho v_x^2 + p + \rho g_x \\ \rho v_x v_y \\ \rho v_x v_z \\ \rho E + p + \rho \mathbf{g} \end{pmatrix}, \quad (4)$$

here  $\mathbf{v} = (v_x, v_y, v_z)^T$  are the speed components,  $\mathbf{g} = (g_x, g_y, g_z)^T = -\nabla \Phi$  is the gravity,  $E = \frac{|\mathbf{v}|^2}{2} + \frac{p}{(\gamma-1)\rho}$  is the total energy, and  $p$  is the pressure. Components  $\mathbf{F}_y$  and  $\mathbf{F}_z$  are obtained similarly [1]. The pressure is presented by barotropic and isothermal equations of state with  $\gamma = 5/3$ .

### 3 Discretization

Many modern high-resolution numerical schemes for gasdynamics conservation laws use the Godunov approach. These methods are also called finite volume methods. They, as a rule, use two-step-by-step methods of type predictor-corrector. Many of them use a uniform grid: cubic or parallelepiped. These schemes utilize the sliding average of the solution  $u(x, y, z, t)$  in  $x$  direction:

$$\bar{u}(x, t) \equiv \frac{1}{|I_x|} \int_{I_x} u(s, t) ds, \quad I_x \equiv \{s : |s - x| \leq \frac{\Delta x}{2}\}$$

so that the integration of the conservation laws (1) over the rectangle  $I_x \times [t, t + \Delta t]$  gives the equivalent formulation:

$$\begin{aligned} \bar{u}(x, t + \Delta t) = & \bar{u}(x, t) - \frac{1}{\Delta x} \left[ \int_{I_x}^{t+\Delta t} f(u(x + \frac{\Delta x}{2}, \tau)) d\tau - \right. \\ & \left. - \int_{I_x}^{t+\Delta t} f(u(x - \frac{\Delta x}{2}, \tau)) d\tau \right]. \end{aligned} \quad (5)$$

Central schemes of the type Lax-Wendroff denote a class of difference methods for solving hyperbolic partial differential equations. The original one involves a strong viscosity and low resolution. Nessyahu and Tadmor [5] proposed a second order accurate scheme with a piecewise constant approximation replaced by linear interpolation. Thus the resolution of Nessyahu and Tadmor scheme is better than the resolution of upwind schemes, and are much more easier to implement than the schemes that use Riemann invariants.

The average value  $\bar{w}_j^n$  may be calculated at a time  $t^n$  in the mesh cell  $I_j \equiv \{x : x_{j-1/2} \leq x \leq x_{j+1/2}\}$ . It is necessary to form a piecewise linear interpolation polynomial with respect to mean values  $\bar{w}_j^n$  at a time  $t^n$  in order to calculate the mean value in the cell  $I_{j+\frac{1}{2}} \equiv \{x : x_j \leq x \leq x_{j+1}\}$  at the time level  $t^{n+1}$ .

A 1-D piece-wise linear approximation may be written as follows

$$w(x, t^n) = \sum [\bar{w}_j^n + w_j' \left( \frac{x - x_j}{\Delta x} \right)] \chi_j(x).$$

Here  $\chi_p(x)$  is a characteristic cell function, but  $w_j'$  is a first order limiter built on mean values of neighbourhood cells  $\{\bar{w}_j^n\}$ . If  $\{\bar{w}_j^n, t \geq t^n\}$  is a conservation laws exact solution  $w_t + f(w)_x = 0$ , then a central difference scheme is obtained versus Godunov's upwind scheme. Let  $\bar{w}_{j+1/2}^n(t) = \frac{1}{\Delta x} \int_{I_{j+1/2}} w(\xi, t) d\xi$  be a mean value shifted to the cell center. Then the control value (5) integrating gives:

$$\begin{aligned} \bar{w}_{j+1/2}^n(t^{n+1}) &= \bar{w}_{j+1/2}^n(t^n) - \\ &- \lambda \left[ \frac{1}{\Delta t} \int_{t^n}^{t^{n+1}} f(w_{j+1}(\tau)) d\tau - \frac{1}{\Delta t} \int_{t^n}^{t^{n+1}} f(w_j(\tau)) d\tau \right]. \end{aligned} \quad (6)$$

Here  $\lambda = \frac{\Delta t}{\Delta x}$  is a common restriction to the time step

Piece-wise linear mean values constructed at time-step  $t = t^n$  give  $\bar{w}_{j+1/2}^n(t^{n+1}) = 1/2(w_{j+1}^n + w_j^n) + 1/8(w_j' - w_{j-1}')$ . It follows easily that  $\frac{1}{\Delta t} \int_{t^n}^{t^{n+1}} f(w_j(\tau)) d\tau \sim f(w_j(t^{n+1/2}))$ . The values

$$w_j^{n+\frac{1}{2}} = \bar{w}_j^n - \frac{\lambda}{2} (f(w_j))' \quad (7)$$

are calculated in the end of the predictor step.

The expression

$$\bar{w}_{j+\frac{1}{2}}^{n+1} = \frac{1}{2}(\bar{w}_j^n + \bar{w}_{j+1}^n) + \frac{1}{8}(w_j' + w_{j+1}') - \lambda \left[ f(w_{j+1}^{n+\frac{1}{2}}) - f(w_j^{n+\frac{1}{2}}) \right] \quad (8)$$

gives a possibility to obtain the values on the corrector step. Here  $w_j'$  and  $f(w_j)'$  are the spatial discrete slopes for the corresponding mesh functions described in [4, 9].

Let the piecewise linear scheme (8) be modified in order to avoid the shift by  $1/2$

$$\bar{w}_j^{n+1} = \frac{1}{4}(\bar{w}_{j-1}^n + 2\bar{w}_j^n + \bar{w}_{j+1}^n) - \frac{1}{16}((w_x)_{j+1} - (w_x)_{j-1}) - \quad (9)$$

$$-\frac{\lambda}{2} \left[ f(w_{j+1}^{n+\frac{1}{2}}) - f(w_{j-1}^{n+\frac{1}{2}}) \right] - \frac{1}{8} ((w_x)_{j+\frac{1}{2}} - (w_x)_{j-\frac{1}{2}}).$$

Consider (9) so that  $(w_x)_j$  and  $(w_x)_{j+\frac{1}{2}}$  are the discrete time derivatives for the  $t^n$  and  $t^{n+1}$  time steps. The value  $w_j^{n+\frac{1}{2}}$  is defined on the predictor step by (7). The Courant-Friedrichs-Levi condition must be fulfilled for the given central difference scheme.

Consider a two-dimensional case, then a piecewise linear approximation  $\bar{w}_{i,j}^n$  is obtained for the mean values corresponding to the cell center  $C_{ij}$ :

$$C_{ij} = \left\{ (\xi, \eta) : |\xi - x_i| \leq \frac{\Delta x}{2}, |\eta - y_j| \leq \frac{\Delta y}{2} \right\}$$

For the predictor step we have the following:

$$w(x, y, t^n) = \sum \left[ \bar{w}_{ij}^n + w'_{ij} \left( \frac{x - x_i}{\Delta x} \right) + \dot{w}_{ij} \left( \frac{y - y_j}{\Delta y} \right) \right] \chi_{ij}(x, y) \quad (10)$$

here  $w'_{ij}$  and  $\dot{w}_{ij}$  are the limiters along x and y axes.

#### 4 Numerical Experiments for High Resolution Schemes. Numerical tests in 2D

Implementing any difference scheme includes a quite important stage – testing. Our code was tested using three test problems in a two-dimensional setting thus the accuracy and robustness could be examined. The first test to implement was a Sedov-Taylor problem. It is a well known and rather severe spherically symmetric shock wave propagation problem. We complicated it by considering an interaction of two spherically symmetric shock waves propagating from two explosion sources of equal power. Thus the oscillations beyond shocks and steep gradients common to this difference scheme may be analyzed.

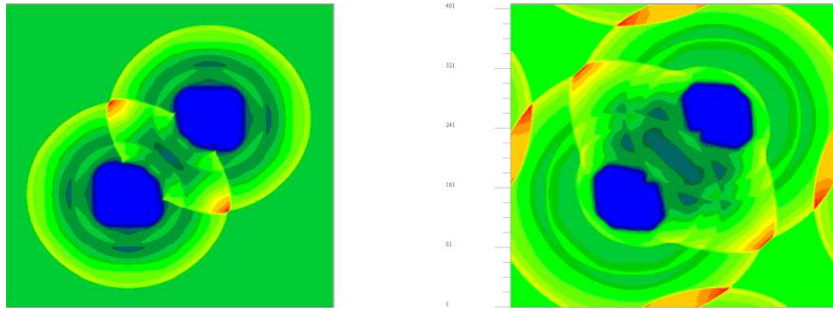
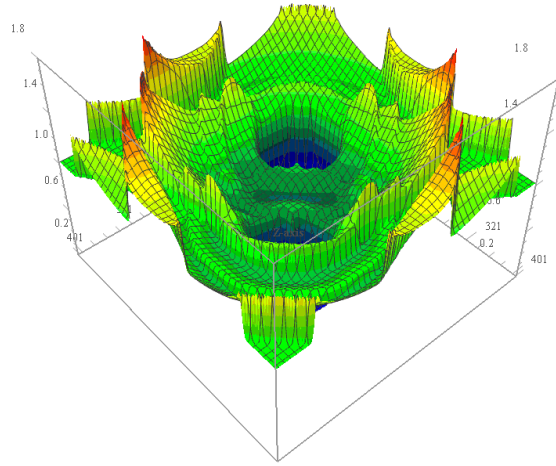


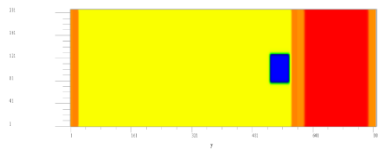
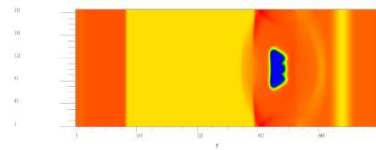
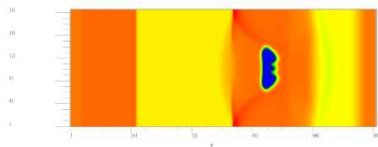
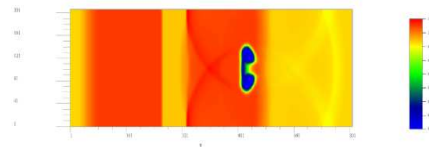
Figure 1. Sedov-Taylor test for interacting shock waves. On the left figure  $t=2.2631$ , on the right  $t=4.6978$

The second test is a shock wave and gas bubble interacting problem. The bubble is considered to be filled in with the gas of low density [6]. And the last test problem, considered in this paper, was taken from [7].

Figure 2. 3D figures for Sedov-Taylor test. Time  $t=4.6978$ 

#### 4.1 Sedov-Taylor test

Consider a rectangular  $400 \times 400$  cell computational domain. Two power sources are situated on its diagonal and equally distanted from the center. Spacial steps are  $dx=0.05$  and  $dy=0.05$ , specific heat ratio is  $\gamma = 1.4$ . The initial values of density and pressure are 1.0 in the whole domain, velocity components are equal to 0. Notice that rectangular grids are noninvariant with respect to rotation. So the difference scheme "quality" can be estimated by obtaining a spherically symmetric shock waves.

Figure 3. Shock waves interacting with gas bubble at time  $t=0.12$ Figure 4. Shock waves interacting with gas bubble at time  $t=2.335$ Figure 5. Shock waves interacting with gas bubble at time  $t=6.586$ Figure 6. Shock waves interacting with gas bubble at time  $t=10.0$

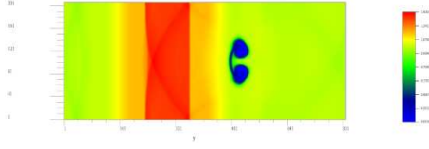


Figure 7. Shock waves interacting with gas bubble at time  $t=14.058$

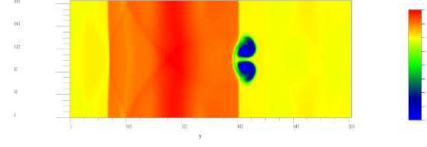


Figure 8. Shock waves interacting with gas bubble at time  $t=18.988$

### 4.2 Bubble test

We simulate the interaction of a low density gas bubble of radius  $r = 0.2$ , centered at  $(0.5, 0)$  with a shock wave. The shock is initially at  $x = 0.2$ , and the initial conditions to the right of the shock and outside the bubble are  $(\rho, u, v, p)^T = (1, 0, 0, 1)^T$ , inside the bubble the pressure and density are  $p = 1$  and  $\rho = 0.1$ , and to the left of the shock, they are determined by the Rankine-Hugoniot conditions [3].

We consider the 2-D Euler equation of gas dynamics in the strip  $R:(-0.5, 0.5)$  with the solid wall boundary conditions prescribed at  $y = \pm 0.5$ . The initial data correspond to a vertical left-moving shock, initially located at  $x = 0.75$ , and a circular bubble with radius 0.25, initially located at the origin. Notice that as the problem was considered for the rectangular grid, then the low density gas domain should be defined for the corresponding rectangular domain. See on the right-hand side in figure 3. These results demonstrate the robustness and stability of the proposed central scheme to evolve the solution of hyperbolic conservation laws. In (3) – (8) the interaction of gas cloud and shock wave at various times is presented.

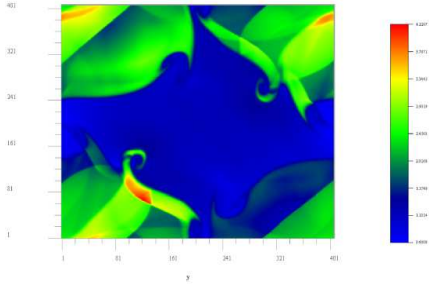


Figure 9. 2D shock tube  $t=0.4564$

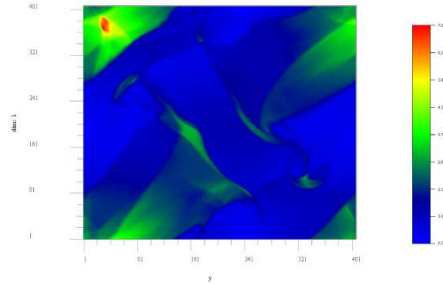


Figure 10. 2D shock tube  $t=0.90947$

### 4.3 Two-dimension shock tube test

Consider (1) 2-D shock tube problem [7, 10]. Computational domain is a square  $R:\{0:1 \times 0:1\}$ , divided into four quadrants by lines  $x = 1/2, y = 1/2$ . Spatial steps are  $dx=0.0025$  and  $dy=0.0025$ , specific heat ratio is  $\gamma = 1.4$ . We denote the quadrants [7]: left lower – 1.1, right lower – 1.2, left top – 2.1,

right top – 2.2 and set a Riemann problem initial data in these quadrants as follows:  $(\rho, u, v, p)^T = (2.0, 0.75, 0.5, 1.0)^T$ ;  $(\rho, u, v, p)^T = (1.0, 0.75, -0.5, 1.0)^T$ ;  $(\rho, u, v, p)^T = (1.0, -0.75, 0.5, 1.0)^T$ ;  $(\rho, u, v, p)^T = (3.0, -0.75, -0.5, 1.0)^T$ .

In Figures (11) – (12)  $\rho$  is the density,  $u$  and  $v$  are the velocity components,

$$E = \rho e + \frac{\rho(u^2 + v^2)}{2}$$

is the total energy per unit volume and  $e$  is the internal energy. Ideal gas law  $p = \rho e(\gamma - 1)$  is used to solve the system of equations that is under consideration.

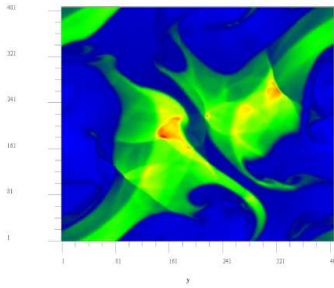


Figure 11.  $t=1.3686$

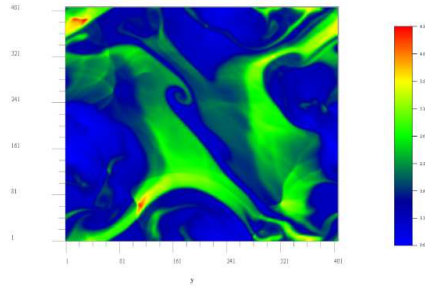


Figure 12.  $t=1.9106$

Figures 9 - 12 present the distribution graphs of the density in the different time steps. Here the number of Courant-Friedrichs-Levi is  $CFL=0.45$ . The results almost coincide with the data obtained in [7]. One may observe that shock fronts are enough sharp and there are not any considerable oscillations beyond them.

#### 4.4 Conclusions

We have presented a difference scheme for solving multidimensional gas-dynamics equations. In particular it has been shown that the scheme and code are able to model the processes governed by conservation laws robustly and accurately. The main purpose of this article was to develop high resolution schemes and to illustrate their potential. Our numerical experiments suggest that these schemes have a good resolution and may be applied for solving various astrophysical problems.

This article has been written under the support of the grant RFFI - Moldova (IKI RAS - IMI ASM) 08.820.06.40 RF.

#### References

- [1] MATSUMOTO T. *Self-gravitational Magnetohydrodynamics with Adaptive Mesh Refinement for Protospellar Collapse*. Publ. Astron. Soc. Japan, **59**, 2007, October 25.
- [2] GHELLER C., PANTANO O., MOSCARDINI L. *A cosmological hydrodynamic code based on the Piecewise Parabolic Method*. Mon. Not. R. Astron. Soc. 5 October 2006.

- [3] JIANG G.-S., LEVY D., LIN C.-T., OSHER S., TADMOR E. *High-Resolution Nonoscillatory Central Schemes With Nonstaggered Grids For Hyperbolic Conservation Laws*. SIAM J. NUMER. ANAL. Vol. 35, No. 6, p. 2147–2168, December 1998.
- [4] RYBAKIN B., SHIDER N. *Computer modeling of multidimensional problems of gravitational gas dynamics on multiprocessor computers*. Computer Science Journal of Moldova, 2009, **17**, No. 1(49), 3–13.
- [5] NESSYAHU H., TADMOR E. *Non-oscillatory central differencing for hyperbolic conservation laws*. J. Comp. Phys., 1990, **87**, 408–448.
- [6] BALBRAS J., QIAN XIN. *Non-oscillatory Central Schemes for 3D Hyperbolic Conservation Laws*. "Hyperbolic Partial Differential Equations, Theory, Numerics and Applications", Proceedings of the 12th international conference, University of Maryland, 2009.
- [7] LEVY D., PUPPO G., RUSSO G. *A Forty-Order Weno Scheme for Multidimensional Hyperbolic System of Conservation Laws*. Mathematical Modelling and Numerical Analysis, 1999, **33**, No. 3, 547–571
- [8] KURGANOV A., CHI-TIEN LIN. *On the Reduction of Numerical Dissipation in Central-Upwind Schemes*. Communications in Computational Physics, 2007, **2**, No. 1, 141–163.
- [9] TOTH G., ODSTRCIL D. *Comparison of Some Flux Corrected Transport and Total Variation Diminishing Numerical Schemes for Hydrodynamic and Magnetohydrodynamic Problems*. Journal of Comp. Phys., 1996, **128**, 82–100.
- [10] LISKA R., WENDROFF B. *Comparison of Several Difference Schemes on 1d and 2d Test Problems for the Euler Equations*. SIAM J. SCI. COMPUT, 2003, **25**, No. 3, 995–1017.
- [11] KULIKOV I., LAZAREVA G., SNYTNIKOV A., VSHIVKOV V. *Supercomputer Simulation of an Astrophysical Object Collapse by the Fluids-in-Cell Method*. Springer-Verlag, Berlin-Heidelberg. V. Malyskin (Ed.): PaCT 2009, LNCS 5698, p. 414–422.

Boris Rybakin, Natalia Shider  
Institute of Mathematics and Computer Science  
Academy of Sciences of Moldova  
Academy street 5, Chishinau, MD-2028  
Moldova  
E-mail: [rybakin@math.md](mailto:rybakin@math.md), [nshider@math.md](mailto:nshider@math.md)

*Received February, 2010*